

GRAIN SIZE DISTRIBUTION EFFECTS ON THE MECHANICAL AND CORROSION BEHAVIOUR OF BIODEGRADABLE METALLIC BIOMATERIALS

C. S. Obayi^{1,2}, Ranna Tolouei², P.S. Nnamchi^{1,4}, N.I. Amalu³, Diego Mantovani²

¹*Department of Metallurgical & Materials Engineering, University of Nigeria, Nsukka, Nigeria.*

²*Laboratory for Biomaterials and Bioengineering,
Department of Materials Engineering & University Hospital Research Centre, Laval University,
Quebec City, G1K 7P4, Canada.*

³*Projects Development Institute, Enugu, Nigeria.*

⁴*Department of Materials Science and Engineering, University of Sheffield, Mapping St,
Sheffield, S1 3JD, United Kingdom.*

ABSTRACT

Maintaining a balance between mechanical and corrosion behaviours is a big challenge in the design and development of metallic biomaterials for biodegradable medical implant application. A current strategy to overcome this challenge is through grain refinement techniques as corrosion rate and mechanical properties of polycrystalline metals are significantly affected by average grain size. Recent studies suggest that grain size distribution (gsd) can also influence dissolution and mechanical behaviours of polycrystalline metals. This work investigated the effect of grain size deviation on the corrosion and mechanical behaviours of pure iron, one of the most studied biometallic materials for biodegradable medical implant application with a view to utilizing the outcome in controlling and adjusting these properties. Thermomechanical processing route of cold rolling and annealing was used to induce different average grain sizes and grain size distributions in pure iron. The grain sizes and gsd were measured with optical microscope. The mechanical properties of yield strength and ductility were evaluated using tensile testing while the corrosion rates were determined in Hank's solution, a near-neutral (pH~7.4) simulated physiological fluid, using weight loss and potentiodynamic polarization methods. The results demonstrate that the corrosion rate decreases and the yield strength increases as the grain size distribution decreases and vice versa. An increase in gsd is accompanied by an increase in residual stress, which lowers strength, but increases corrosion rate due to more active sites of low activation energy. This finding could enable the optimization of mechanical and corrosion properties of biodegradable metallic biomaterials.

Keywords: *grain size distribution, cold rolling, annealing, mechanical properties, corrosion behaviour.*

1.0 INTRODUCTION

Biodegradable metals are used for making temporary medical implants such as stents, deployed for treatment of severe cardiovascular diseases and other ailments. They are intentionally designed to corrode in physiological media and to disappear via corrosion after providing temporary mechanical support during the healing process of a diseased tissue or organ [1]. Materials used for making cardiovascular stents must possess a combination of adequate strength, ductility and biocompatibility [2]. Their corrosion rate is required to match tissue healing rate without compromising its mechanical integrity and metabolic reactions of the human body during the healing process.

Maintaining a balance between corrosion rate and mechanical properties (strength, ductility) is a big challenge in the design and development of metallic biomaterials for biodegradable medical implant application as their precursor implants were not originally designed to degrade in the implant sites, but to be permanent, corrosion resistant and inert. One of the most investigated candidate metals for making biodegradable metallic implants is pure iron (Fe) and its alloys; alloyed with few available nontoxic elements to the human body such as Ca, Zn, Mn, P, small quantities rare-earth metals [3]. There is a current trend in the biodegradable metal research community to adjust and control the

degradation of behaviour of biometals through grain refinement techniques. Moravej, et al [4] and Nie, et al [5], used electrodeposition and severe plastic deformation (ECAP) techniques respectively to grain refine pure Fe and adjust its corrosion rate and biocompatibility in physiological media. Corrosion rate and mechanical properties of polycrystalline metals are significantly affected by average grain size. As the yield strength of pure Fe varies inversely with the square root of the average grain diameter according to well-known Hall-Petch relation, its corrosion rate has been found to decrease as average grain size decreases in physiological media [5, 6]. Besides the above effect of mean grain size on mechanical and corrosion behaviours of polycrystalline metals, grain size distribution (gsd) or difference in the distribution of the size of grains or diversity in the size of grains has been found to equally influence these properties. Kurzydowski [7] found through stochastic model that the flow stress of polycrystals is a function of both the mean and the standard deviation of the distribution function of size of grains. The yield strength of a polycrystal decreases with an increase in the value of the standard deviation of grain size distribution. Berbenni, et al [8], equally found through theoretical micromechanical model using unimodal log-normal distributions that the overall yield strength of fine grained metal depends not only on mean grain size but also on the dispersion of the distribution. A decrease in yield stress and increase in internal stresses with increase in the dispersion occurs, especially when the mean grain size is on the micron range [8]. A relationship between corrosion current (corrosion rate) and grain size distribution has been proposed by Srikant Gollapudi [9]. The relation (equation 1) is as follows:

$$i_{uc} = A + B(\bar{d})^{\frac{1}{2}} \exp\left(-\frac{9}{8}S_n^2\right) \quad (1)$$

where i_{uc} is corrosion current density, A and B are constants whose values depend on the material (composition or impurity level) and on the nature of the media respectively; values of A and B can be obtained from corrosion studies carried out as a function of grain size in pure metals, \bar{d} is the mean grain size and S_n is the standard deviation, a measure of grain size distribution. This relation implies that as the grain size distribution increases or becomes broader, the corrosion rate of a metal could decrease in a non-passivating environment while it could increase in a passivating environment and vice versa.

This work is aimed at assessing the effect of gsd on corrosion and mechanical behaviour of pure iron with a view to utilizing the outcome in controlling and adjusting these properties for biodegradable medical implant application. This study will add to the emerging knowledge on the influence of microstructure on the corrosion behaviour of pure Fe as biodegradable metallic implant material.

2.0 EXPERIMENTAL DETAILS

2.1 Materials

The material used in this work was an Armco[®] soft ingot iron (>99.8% purity) in the form of 2 mm thick as-rolled sheets (Good fellow Limited, Cambridge, United Kingdom). The chemical composition of as-received material was determined in a previous work [6] and is given in Table 1. The chemicals for preparing the test solution (Hanks' solution) were purchased in the form of powders. They include Hanks modified salt (H1387, Sigma Aldrich, USA), HERPES acid (H3375, Sigma Aldrich, Canada); sodium bicarbonate (SX0320-1, Merck KGaA, Germany) and HERPES sodium salt (DB0265, Bio Basic, Canada).

Table 1: Chemical composition of the as-received Armco pure iron

Element	C	Ni	Cr	Mn	Cu	Mo	S	Sn	P	Si	Al	Fe
Weight %	0.006	0.037	0.032	0.041	0.017	0.002	0.014	0.014	0.019	0.008	0.010	Balance

2.2 Cold rolling and annealing

Samples were cut from the 2 mm-thick pure iron sheets and cold rolled to 75% (UD 75% CR) and 85% (UD 85% CR) thickness reduction to achieve 0.5 mm and 0.3 mm thickness, respectively. Rolling was unidirectional with reduction in thickness limited to 0.2 mm per pass at a rolling speed of 32 r.p.m on a Stanat two-high rolling mill (Stanat, Rolling Mill; model TA-315), using 130 mm work rolls. In order to induce different grain sizes, the UD cold-rolled samples were annealed in a tube furnace under a high purity argon atmosphere using a heating rate of 6.5°C per minute to 550°C, 800°C, 1000°C, soaked for one hour and furnace cooled.

2.3 Microstructure and grain size measurement.

The microstructure and grain size of the as-received, cold-rolled and annealed pure iron samples were observed on the rolling surface and determined using an optical microscope (Nikon Epiphot 200, Japan) equipped with CLEMEX Vision image analyzer (Clemex, Longueuil, Canada). The image analyzer enabled the determination of the minimum and maximum grain sizes, the average grain size and the standard deviation (gsd). Prior to microstructural examination and grain size measurement, the samples were cut and mounted in acrylic resin and wet ground with 320-1000 grit SiC papers and finally polished with 6µm and 1µm diamond suspension and 0.05 µm alumina paste. They were then etched using a 2% Nital solution to delineate the grains and grain boundaries.

2.4 Mechanical properties

Subsize dog-bone-shaped tensile specimens having a gauge length of 25 mm, width of 6.38 mm, total length of 100 mm and thicknesses of 2 mm for the as-received Fe and thickness of 0.5 and 0.3 mm, respectively, for the rolled and annealed samples, were machined along the rolling direction following the ASTM E8 standard [10]. Tensile tests were carried out at a strain rate of 0.033mm⁻¹ using computer-controlled universal testing machine (SATEC T2000, USA).

2.5 Corrosion behaviour

Static immersion and potentiodynamic polarization tests were used as in vitro experiments to assess the biodegradation behaviour of samples in a modified Hanks' solution; the medium ionic composition and concentration are close to those of human blood plasma. The composition of the prepared Hanks' solution was presented in Ref [11].

The sample sizes for the static immersion test were 20×10×2 mm³, 20×10×0.5 mm³ and 20×10×0.3 mm³ for the as-received and treated samples respectively. They were wet ground using SiC papers from 120 down to 4000 grit, and then were cleaned with ethanol, dried and weighted. Each specimen was suspended in a separate 80 ml-beaker of Hanks' solution maintained at a temperature of 37°C for 14 days (336 hours). After 14 days, the specimens were removed from the Hanks' solution, rinsed with distilled water and ethanol, dried and weighed. The average corrosion rate (ACR) was calculated based on the mass loss using equation (2) from ASTM G31 standard [12].

$$ACR = 8.76 \times 10^4 \frac{W}{A.t.\rho} \quad (2)$$

where *ACR* is the average corrosion rate in millimetre per year (mm/yr), *W* is the mass loss in grams (g), *A* is the exposed surface area (cm²), *t* is the time of exposure in hours and *ρ* is the density of the material (7.87 g/cm³ for Fe).

The potentiodynamic polarization test was performed in a three-electrode cell (VersaSTAT3 potentiostat/galvanostat system, Princeton Applied Research, USA). The setup consisted of a saturated calomel electrode (SCE), a graphite counter electrode and the sample as the working electrode. All potentials are quoted relative to the SCE scale. Each corrosion test was performed in 650 ml of Hanks' solution having a pH of 7.4. The solution was stirred and the temperature was maintained at 37±1°C by a heating jacket during the corrosion tests. For the potentiodynamic tests disc-shaped samples having a surface area of Ø 1.3 cm² were cut, wet ground using SiC papers from 120 down to 4000 grit and subsequently

cleaned with ethanol and dried. The actual circular area of the working electrodes exposed to the solution was 0.16 cm². The potentiodynamic polarization test was carried out at a scanning rate of 0.166 mV.s⁻¹ in the potential range -1000 mV (vs. SCE) to -250 mV (vs. SCE). The open circuit potential (OCP) measurement was maintained up to 1 hr. The corrosion rate (CR) was calculated using equation (3) based on ASTM G59 [13].

$$CR = 3.27 \times 10^{-3} \frac{i_{corr} \cdot EW}{\rho} \quad (3)$$

where CR is the corrosion rate in millimetre per year (mm/yr), i_{corr} is the corrosion current density ($\mu\text{A}/\text{cm}^2$) deduced from Tafel curves, EW is the equivalent weight (27.92 g/eq for Fe) and ρ is the density (g/cm^3).

3.0 RESULTS AND DISCUSSION

3.1 Microstructure, grain size and gsd.

The grain size evolution of the as-received pure Fe and some of the selected cold-rolled and annealed pure Fe samples is shown in Table 2 while their micrographs and grain size distributions are shown in Figure 1. Optical microscopy of the as-received and treated Fe samples, revealed fully equiaxed ferritic microstructures. After annealing, the

treated Fe samples displayed increased mean recrystallized grain sizes and broader grain size distributions with increasing annealing temperatures. The 85%UR-550 has the smallest mean recrystallized grain size and smallest gsd while 85%UR-1000 has biggest grain size and broadest gsd.

3.2 Mechanical properties

The tensile properties of the annealed samples as a function of gsd are shown in Table 3. The yield strengths of the samples decreased with increase in gsd. The yield strengths are also grain size dependent. The 85%UR-550 has the smallest gsd and the highest yield strength, followed by 75%UR-800 and 85%UR-1000. 85%UR-1000 has the highest gsd of 28 μm and lowest yield strength and % elongation (ductility). This is agreement with results of the models by [7] and [8], where the flow stress or yield stress of polycrystals is found to be a function of both the mean and the standard deviation of the distribution function of size of grains. This is because a broader gsd is accompanied with increase in internal stresses and consequently lowers the yield strength and ductility of metals [8].

Table 2: Grain evolution of selected pure iron samples as a function of annealing temperature.

Sample identification	Average grain size (μm)	Grain size distribution, S_n (μm)	Minimum grain size (d_{min}) (μm)	Maximum grain size (d_{max}) (μm)	Grain size range $\Delta d = d_{max} - d_{min}$ (μm)	Annealing temperature
As-received	29.6	4	1.8	134.4	132.6	-
85%UR-550	14.1	1.3	1.8	53.7	51.9	550°C / 1h
75%UR-800	28.1	2.9	3.2	78.4	75.2	800°C / 1h
85%UR-1000	164.6	28	19.2	769.8	750.6	1000°C / 1h

Material	Average grain size (μm)	Grain size distribution, S_n (μm)	Grain size range (μm)	Yield strength (MPa)	Tensile strength (MPa)	% elongation
As-received	29.6	4	132.6	170 ± 2	270 ± 5	49.3±3
85%UR-550	14.1	1.3	51.9	216 ± 13	287 ± 7	46.1±4
75%UR-800	28.1	2.9	75.2	158 ± 2	238 ± 5	49.4±3
85%UR-1000	164.6	28	750.6	93 ± 9	173 ± 17	17.2±2

Table 3: Mechanical properties of the as-received and annealed pure samples and gsd parameters

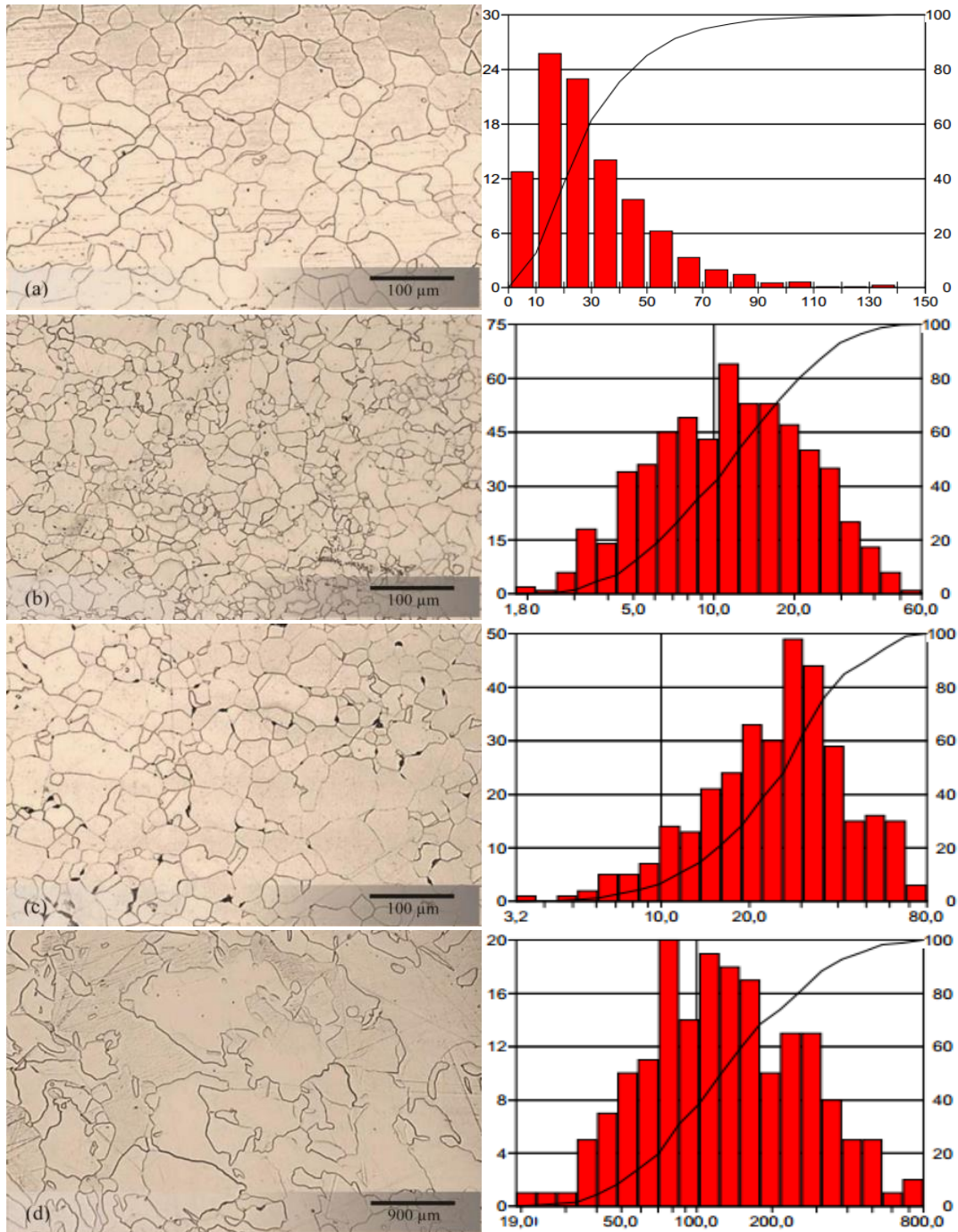


Fig.1: Micrographs and grain size distribution of pure iron: (a) as-received, (b) 85% cold rolled, annealed at 550°C, (c) 75% cold rolled, annealed at 800°C and (d) 85% cold rolled, annealed at 1000°C.

3.3 Corrosion Behaviour

The average corrosion rates of as-received and treated samples based on weight loss method and potentiodynamic polarization methods are shown in Table 4. Their corrosion rates in both static and potentiodynamic polarization tests increased slightly with increase in gsd. The 85%UR-1000 has the highest gsd of 28 μm and

highest corrosion rate, followed by the as-received, 75%UR-800 and 85%UR-550 with gsd of 4, 2.9 and 1.3 microns, respectively.

This increase in corrosion rates can be attributed to internal stresses as increase in the grain dispersion is accompanied by increase internal stresses [8] and corrosion rate of metals are significantly affected by

internal residual stresses [14]. An increase in residual stress leads to more active sites of low activation energy [15, 16, 17]. It generally increases corrosion either from enhanced cathodic reactions, increased anodic dissolution (more initiation sites coupled with increased surface activity), or the creation of a defective oxide. The 85%UR-550 sample has the lowest gsd and therefore, the lowest residual stress and lowest corrosion rate. The increase in corrosion rates of the Fe samples as the

grain size distributions become broader in near-passivating physiological environment is in agreement with the proposal by Gollapudi [9]. The corrosion rates of the annealed Fe samples are also grain-size dependent.

The cumulative effect of gsd on the yield strengths and corrosion current densities of the treated pure Fe samples is shown in Figure 2. The yield strength decreased while corrosion current density increased with increase in gsd.

Table 4: Average corrosion rates based on weight loss method, corrosion current densities, potentials and calculated corrosion rates based on potentiodynamic polarization method.

Material	Average grain size (μm)	Grain size distribution, S_n (μm)	Grain size range (μm)	Average corrosion rate based on weight loss (mm/yr)	$I_{\text{corr}}(\mu\text{A}/\text{cm}^2)$	Potential i (mV)	Corrosion rate based on potentiodynamic polarization method (mm/yr)
As-received	29.6	4	132.6	0.138 \pm 0.011	20.89 \pm 0.617	-732 \pm 3	0.242 \pm 0.013
85%UR-550	14.1	1.3	51.9	0.120 \pm 0.006	14.887 \pm 0.921	-724 \pm 4	0.172 \pm 0.012
75%UR-800	28.1	2.9	75.2	0.127 \pm 0.003	18.50 \pm 0.704	-735 \pm 11	0.215 \pm 0.043
85%UR-1000	164.6	28	750.6	0.146 \pm 0.007	21.056 \pm 2.63	-740 \pm 8	0.244 \pm 0.031

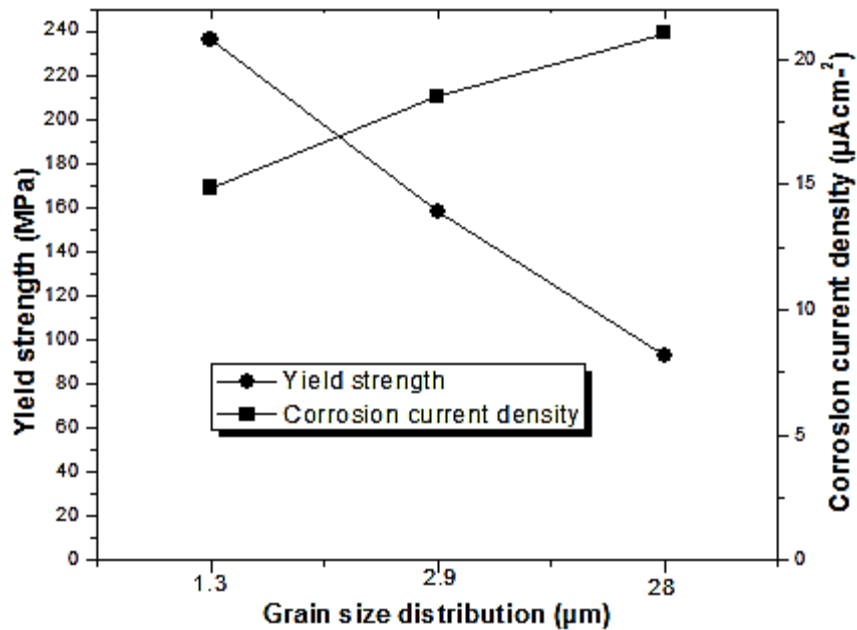


Fig. 2: Yield strength and corrosion current density versus grain size distribution.

4.0 CONCLUSION

Yield strength of the treated pure Fe samples is a function of both the grain size distribution and mean grain size; decreasing with increase in both grain size distribution and average grain sizes. The corrosion rates in both static and potentiodynamic polarization corrosion tests increased slightly with increase in grain size distribution in simulated physiological medium. Since yield strength decreases and corrosion rate increases with increase in grain size distribution, strength and corrosion rate of biodegradable metals could be optimized as a function of both the grain size distribution and average grain sizes.

ACKNOWLEDGEMENTS

The authors would like to thank the Canadian Commonwealth Scholarship Program and University of Nigeria for scholarship award to the first author. This research was partially funded by Natural Science and Engineering Research Council of Canada, Canada Research Chair Program and CHU de Quebec Research Center. The Authors are also grateful to Marc Choquette, Maude Larouche and Daniel Marcotte, from the Department of Mining, Metallurgical and Materials Engineering, Laval University, Quebec City, Canada, for their technical support, help and guidance.

REFERENCES

1. R. Waksman; R. Pakala; R. Baffour; R. Seabron; D. Hellinga; F.O. Tio. *Short-Term Effects of Biocorrosible Iron Stents in Porcine Coronary Arteries*. Journal of Interventional Cardiology, 2008, **21**(1): 15-20.
2. Hermawan H, Mantovani D. *Process of prototyping coronary stents from biodegradable Fe-Mn alloys*. Acta Biomaterialia 2013;9:8585-92.
3. Song, G., *Control of biodegradation of biocompatible magnesium alloys*. Corrosion Science, 2007. **49**(4): p. 1696-1701.
4. Moravej, M., et al., *Effect of electrodeposition current density on the microstructure and the degradation of electroformed iron for degradable stents*. Materials Science and Engineering: B, 2011. **176**(20): p. 1812-1822.
5. F.L. Nie; Y.F. Zheng; S.C. Wei; C. Hu; G. Yang. *In vitro Corrosion, Cytotoxicity and Hemocompatibility of Bulk Nanocrystalline Pure Iron*. Biomedical Materials. 2010, 5(6), p.065015.
6. Camillus Sunday Obayi, Ranna Tolouei, Afghany Mostavan, Carlo Paternoster, Stephane Turgeon, Daniel Oray Obikwelu, Boniface Adeleh Okorie, Diego Mantovani, *Effect of Grain Sizes on Mechanical Properties and Biodegradation Behaviour of Pure Iron for Cardiovascular Stent Application*, Biomatter 2014; 4:e32201.
7. K.J.Kurzydowski, A model for the flow stress dependence on the distribution of grain size in polycrystals, Scripta Metallurgica, 1990. Vol. 24, pp. 879-883.
8. S.Berbeni, V.Favier, M.Berveiller, *Impact of the grain size distribution on the yield stress of heterogeneous materials*, International Journal of Plasticity, 2007. 23: p. 114-142.
9. Gollapudi, S., *Grain size distribution effects on the corrosion behaviour of materials*. Corrosion Science, 2012. **62**: p. 90-94.
10. ASTM, *Standard Test Methods for Tension Testing of Metallic Materials*. 2013.
11. Lévesque J, Hermawan H, Dubé D, Mantovani D. Design of a pseudo-physiological test bench specific to the development of biodegradable metallic biomaterials. Acta Biomaterialia 2008;4:284-95.
12. ASTM, *Standard Guide for Laboratory Immersion Corrosion Testing of Metals*. 2012.
13. ASTM, *Standard Test Method for Conducting Potentiodynamic Polarization Resistance Measurements*. 2009.
14. Ralston, K. and N. Birbilis, *Effect of grain size on corrosion: a review*. Corrosion, 2010. **66**(7): p. 075005-075005-13.
15. U.R. Evans, *The Corrosion and Oxidation of Metals: First Supplementary Volume*, 1968, Edward Arnold Ltd, London, p. 149.
16. Forouli, Z.A. and H.H. Uhlig, *Effect of Cold-Work on Corrosion of Iron and Steel in Hydrochloric Acid*. Journal of the Electrochemical Society, 1964. **111**(5): p. 522-528.
17. N.D. Greene, G. Saltzman, *Effect of Plastic Deformation On the Corrosion of Iron and Steel*. Corrosion, 1964, Vol. 20, No. 9, pp. 293t-298t.